Electronic Supplementary Material (ESI) for RSC Applied Interfaces.

Upcycled Graphene Nanoplatelets Integrated Fiber-based Janus Membranes for Enhanced Solar-driven Interfacial Steam Generation

Jalal Karimzadeh Khoei[1,2,+], Mohammad Sajad Sorayani Bafqi[1,2,3,+], Kuray Dericiler[1,3], Omid Doustdar[4], Burcu Saner Okan[1,3], Ali Koşar[1,2,,5,*,] Ali Sadaghiani[1,2,5,] **

[1] Faculty of Engineering and Natural Sciences (FENS), Sabanci University, Orhanli, 34956, Tuzla, Istanbul, Turkey
[2] Sabanci University Nanotechnology and Application Center (SUNUM), Sabanci University, Orhanli, 34956, Tuzla, Istanbul, Turkey
[3] Sabanci University Integrated Manufacturing Technologies Research and Application Center & Composite Technologies Center of Excellence, Manufacturing Technologies, Istanbul, Turkey
[4] Department of Mechanical Engineering, School of Engineering, University of Birmingham, Birmingham, B15 2TT, UK
[5] Center of Excellence for Functional Surfaces and Interfaces for Nano-Diagnostics (EFSUN), Sabanci University, Orhanli, 34956, Tuzla, Istanbul, Turkey
+ These authors contributed equally.
* Correspondence: kosara@sabanciuniv.edu
** Correspondence: a.sadaghiani@sabanciuniv.edu

S1. Characterization results:

The GNP obtained from recycled waste tires was supplied by NANOGRAFEN Co. The Upcycling GNP process comprises two distinct stages: the pyrolysis step and the conversion of the resulting carbon black into Graphene Nanoplatelets (GNP). This step demonstrates a high yield of 75%.

S1.1. GNP characteristics:

Elemental analysis (XPS)

C (at%): 87, O (at%): 9, Fe (at%): 0.5 and other (at%): 3.5

Sample	C1s			O1s			Fe2p		
	Group	Binding Energy (eV)	Peak Intensity (a.u.)	Group	Binding Energy (eV)	Peak Intensity (a.u.)	Group	Binding Energy (eV)	Peak Intensity (a.u.)
GnP-recycled	C=C	284.1	264,962	C-O, Fe-O	531.1	31,801	$Fe2p_{3/2}$	711.3	42,571
	C-C	284.8	89,952	C=O	532.6	35,546	Satellite	719.6	40,325
	C-O	286.2	26,325				$Fe2p_{1/2}$	725	41,908
	O-C=O	289.1	14,875				Satellite	729.8	40,769

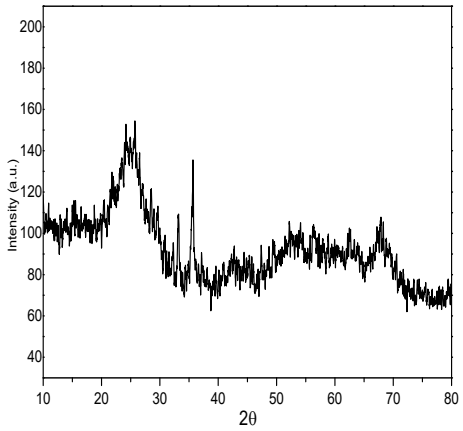

Figure S 1. XRD spectrum of graphene nanoplatelets (GNP)

There is a broad peak at 2Θ=25.5˚attributed to the (002) reflection of the graphitic plane. The peaks at 2Θ=35.8˚ belong to the (311) reflection of the Fe catalyst [1,2].

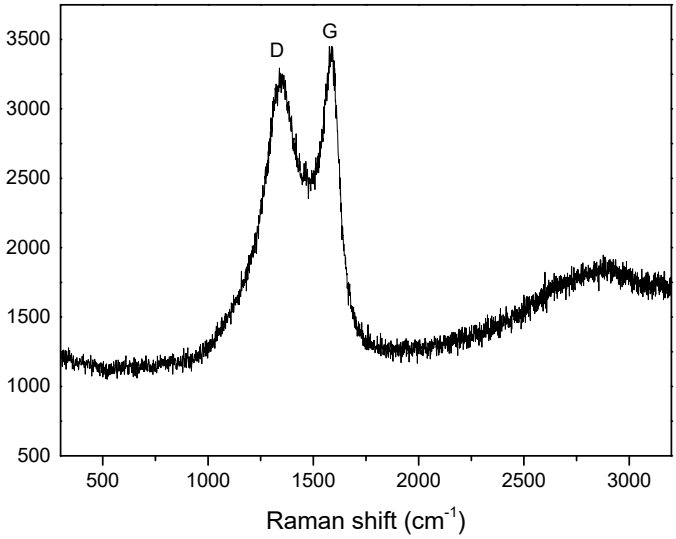

Figure S 2. Raman spectrum of GNP. Raman characterization provides information about crystallite size, presence of sp2-sp3 hybridization, chemical impurities, and defects in the structure.

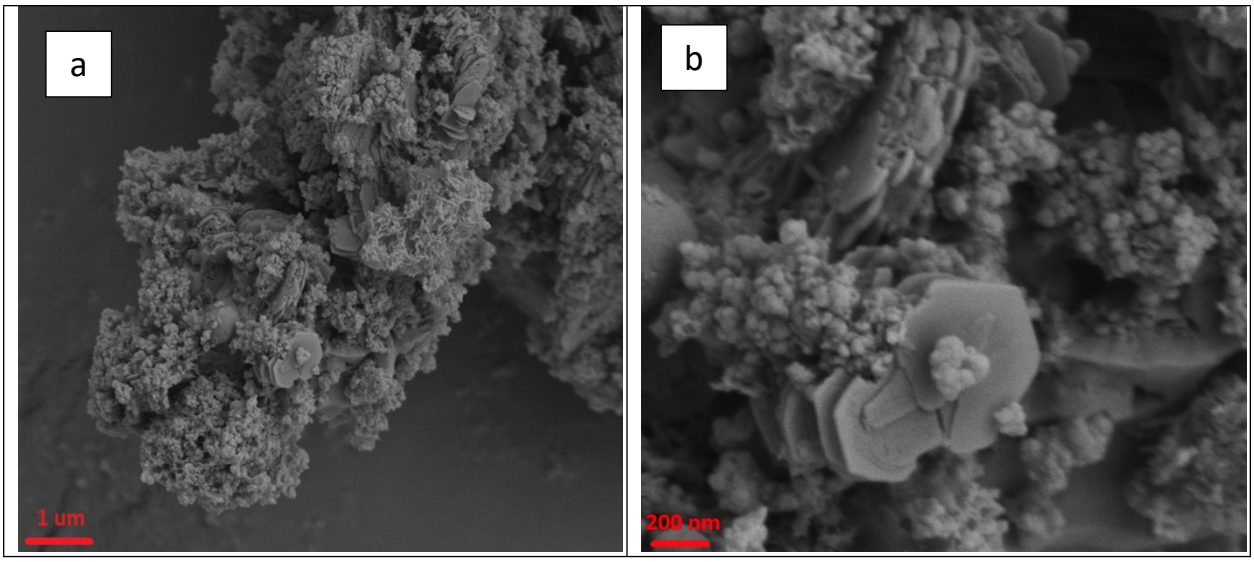

Figure S 3. SEM images of GNP at (a) 25K magnification and (b) 100K magnification. The mean thickness of the GNP platelet is 14 nm, as measured by ImageJ software. The width and length measured as 524 nm and 869 nm, respectively.

S1.2. XRD of PMMA and PMMA/GNP:

XRD analysis was carried out to examine the structural characterization of the nanocomposite and the effect of the GNP nanoparticles on PMMA nanofibers. XRD diffraction patterns for PMMA and PMMA/GNP nanofiber layers are presented in **Figure S3**. A strong, sharp diffraction peak around 30.8° represents the (311) reflection of the Fe catalyst [3,4]. Additional smaller peaks can be distinguished at 44.6° (100) and 55.7° (004). The increased intensity of the diffraction, followed by increasing the concentrations of GNP, is attributed to the more significant number of stacked graphene layers. In addition to the mentioned peak, a characteristic peak at 25.5° 5˚is attributed to the (002) reflection of the graphitic plane that can barely be seen at 0.5%wt GNP concentration. An increase in the diffraction peak intensity due to the (002) diffraction plane implies an increased crystallinity in the samples. Thus, it can be inferred that the increased concentration of GNP causes a slight increase in the crystallinity of the fabricated layers.

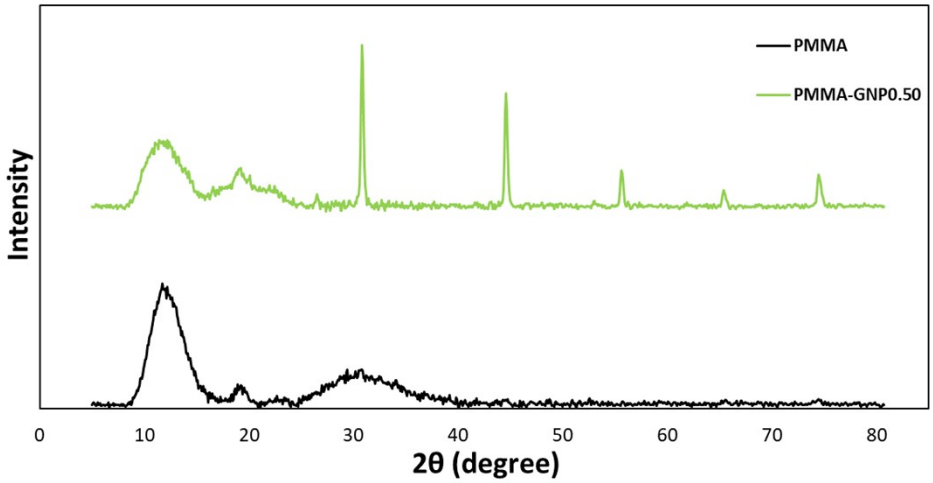

Figure S3. XRD results of PMMA, and PMMA/GNP

S1.3. TGA of PMMA, GNP and PMMA/GNP:

TGA analysis of the GNP, PMMA nanofiber, and PMMA/GNP0.5%wt are represented in **Figure S3**. As it can be seen, results show that PMMA nanofibers begin to degrade when heated near their melting point, and a slight loss of mass occurs from about 100°C due to the release of water. A dramatic weight loss begins from 280°C. The weight loss reaches almost 0% at 400°C. This amount is less than that of PMMA/GNP0.5%wt. The use of GNP slightly improves the thermal stability of the layers. It should be considered that the thermal stability around the usage temperature of the membrane is important, and all prepared samples have excellent stability until 200°C.

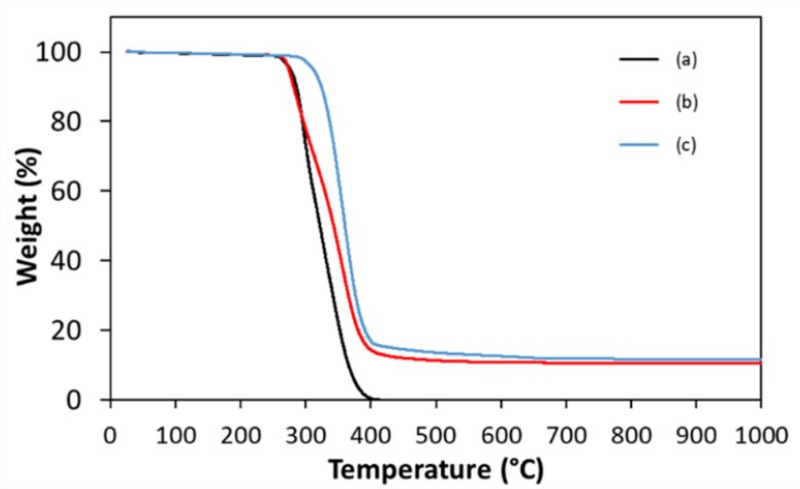

Figure S3. TGA curve of GNP, PMMA, and PMMA/GNP

S1.4. Contact angle of PAN, PMMA, PMMA/GNP:

The static contact angles of PAN, PMMA, and PMMA/GNP0.5%wt electrospun nanofibers were measured using distilled water droplets at room temperature, and the measurements are demonstrated in **Figure S4**. According to the contact angle measurements of PAN (5.4°) and the PMMA (120.3°), the PAN membrane has a hydrophilic structure, and the PMMA-based mat is a hydrophobic membrane. PAN polymer chemical structure represented nucleophile –CN substitution on its surface. Therefore, PAN has a high polarity, which causes water attraction [5]. On the other hand, the PMMA chemical structure includes both hydrophobic $–CH_3$ groups and -COOR hydrophilic groups. As mentioned before, the contact angle measurement of the PMMA electrospun membrane suggests that in the electrospinning process, most of the hydrophilic groups (-COOR) rotate underneath the surface inside the fiber; meanwhile the hydrophobic groups ($–CH_3$) move onto the surface of the fibers [6]. Upon the addition of 0.5 wt.% GNP to the PMMA nanofibers, the contact angle increased to 140.8° for PMMA/GNP0.5%. The GNP also improves the hydrophobic properties of the PMMA nanofibrous layer.

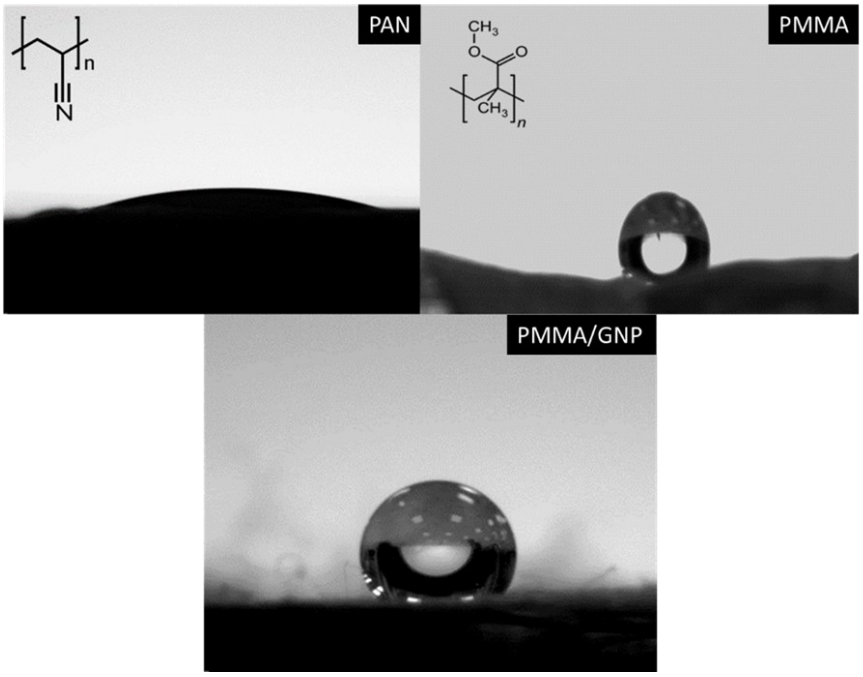

Figure S4. Contact angle of PAN, PMMA, and PMMA/GNP

S2. Stability of the Janus membranes:

An investigation was conducted to observe the stability of the Janus membranes when being exposed to pure water after 24 hours. The SEM images of the PMMA/GNP and PAN layer (Figure S5) indicate that the samples did not undergo any morphological changes before and after the exposure.

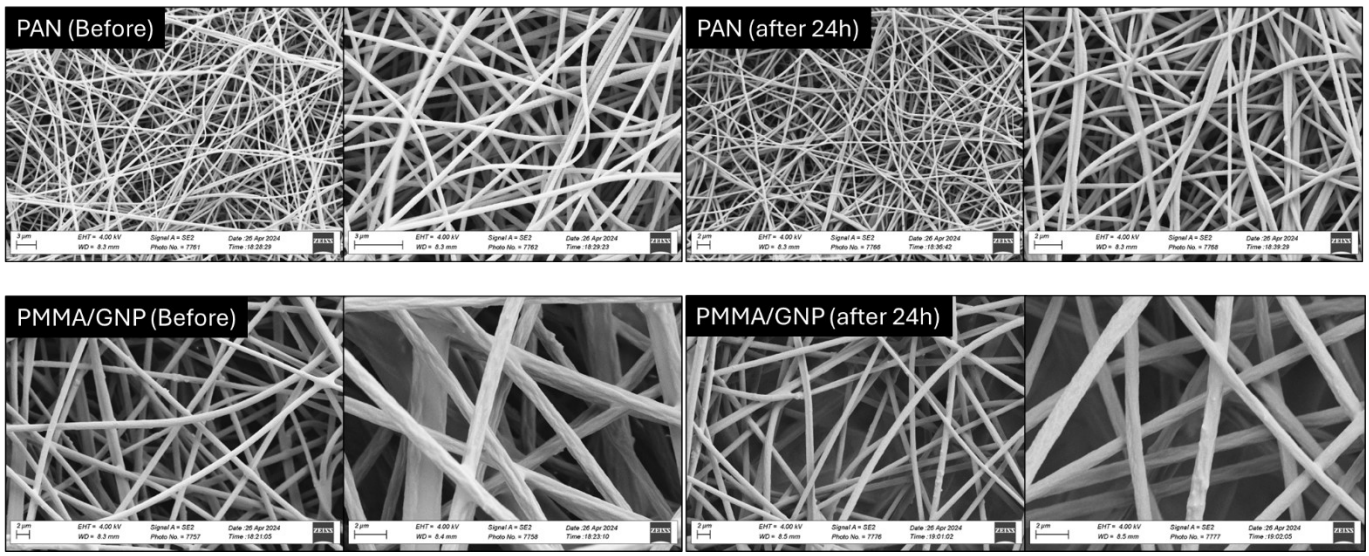

Figure S5. SEM images of PAN and PMMA/GNP before and 24 hours after the exposure to pure water

References

1. Siddheswaran, R., Manikandan, D., Avila, R.E., Jeyanthi, C.E., and Mangalaraja, R.V. (2015). Formation of carbon nanotube forest over spin-coated Fe2O3 reduced thin-film by chemical vapor deposition. Fullerenes, Nanotubes and Carbon Nanostructures *23*, 392-398.
2. Okan, B.S., Yurum, A., Gorgülü, N., Gürsel, S.A., and Yurum, Y. (2011). Polypyrrole coated thermally exfoliated graphite nanoplatelets and the effect of oxygen surface groups on the interaction of platinum catalysts with graphene-based nanocomposites. Industrial & engineering chemistry research *50*, 12562-12571.
3. Poudeh, L.H., Okan, B.S., Zanjani, J.S.M., Yildiz, M., and Menceloglu, Y. (2015). Design and fabrication of hollow and filled graphene-based polymeric spheres via core–shell electrospraying. RSC advances *5*, 91147-91157.
4. Siddheswaran, R., Manikandan, D., Avila, R.E., Jeyanthi, C.E., and Mangalaraja, R.V. (2015). Formation of carbon nanotube forest over spin-coated Fe2O3 reduced thin-film by chemical vapor deposition. Fullerenes, Nanotubes & Carbon Nanostructures *23*, 392-398.
5. Yalcinkaya, F., Yalcinkaya, B., Pazourek, A., Mullerova, J., Stuchlik, M., and Maryska, J. (2016). Surface modification of electrospun PVDF/PAN nanofibrous layers by low vacuum plasma treatment. International Journal of Polymer Science *2016*.
6. Ma, Y., Cao, X., Feng, X., Ma, Y., and Zou, H. (2007). Fabrication of super-hydrophobic film from PMMA with intrinsic water contact angle below 90. Polymer *48*, 7455-7460.